A&A manuscript no.
(will be inserted by hand later)

Your thesaurus codes are:
06 (08.03.4; 08.06.2; 08.16.5; 13.09.6)

ASTRONOMY
AND
ASTROPHYSICS
27.9.1996

SWS H_2 observations in the BD+40°4124 group *

P.R. Wesselius[1], **M.E. van den Ancker**[2], **E.T. Young**[3], **F.O. Clark**[4], **T. Prusti**[5], **P.R. Roelfsema**[1], **C. Waelkens**[6], **D.H. Wooden**[7], **D.R. Boxhoorn**[1,5], **A.M. Heras**[5], **E. Huygen**[6], **D.J.M. Kester**[1], and **F. Lahuis**[1,5]

[1] SRON, P.O Box 800, NL-9700 AV Groningen, The Netherlands
[2] Astron. Inst. "Anton Pannekoek", Univ. of Amsterdam, Kruislaan 403, NL-1098 SJ Amsterdam, The Netherlands
[3] University of Arizona, Steward Observatory, Tucson, AZ 85721, U.S.A.
[4] Phillips Laboratory, OL-AA, PL/GOB, Hanscom AFB, MA 01731, U.S.A.
[5] ESA Villafranca, P.O. Box 50727, E-28080 Madrid, Spain
[6] Instituut voor Sterrenkunde, Katholieke Universiteit Leuven, Celestijnenlaan 200B, B-3001 Heverlee, Belgium
[7] NASA Ames Research Center, MS N-245-6, Moffet Field, CA 94035-1000, U.S.A.

Received ; accepted

Abstract. We report the detection of pure rotational lines of H_2 observed in the direction of three young stellar objects in the BD+40°4124 group, with the short-wavelength spectrometer (SWS) on board ISO. The rotational population distributions of all three stars are consistent with a thermal distribution. The derived kinetic temperatures are ≈ 500 K for BD+40°4124 and LkHα 224 and ≈ 800 K for LkHα 225. The amounts of molecular hydrogen detected are 0.01 to 0.04 $M_\odot$. The relative abundances of ortho- and para-hydrogen are consistent with a high temperature equilibrium distribution. We conclude that the molecular hydrogen emission in all three regions appears to lie behind approximately 10–25$^{\rm m}$ of visual extinction and is probably not directly associated with any of the optical sources.

Key words: Circumstellar matter – Stars: Formation – Stars: Pre-main sequence – Infrared: Stars

1. Introduction

BD+40°4124 (= V1685 Cyg) is one of the original Ae/Be stars with associated nebulosity studied by Herbig (1960). It is located in the Cygnus arm at a distance of about one kpc and is the optically brightest member of a small group of young stars that includes LkHα 224 (= V1686 Cyg) and LkHα 225 (= V1318 Cyg), all of which have infrared excesses (Strom et al. 1972). These objects were also studied by Cohen (1972) who concluded that these stars must be very young. The IRAS survey showed a powerful source at this position, but the IRAS positional uncertainty does not allow to assign the flux to one of these three objects; indirect arguments may be used (Hillenbrand et al. 1992; Weaver & Jones 1992).

Aspin et al. (1994) have shown LkHα 225 to be a triple system oriented north-south with the most northern and southern components separated by 5″. They also obtained an 800 μm continuum map of the region that clearly peaks on LkHα 225. Photometric and spectroscopic observations by the same authors strongly suggest that the southern component of LkHα 225 is dominant in the mid-infrared. In particular, it is the brightest member of the group at 10 μm. Interestingly, their K-band spectrum of LkHα 225-South shows strong vibration-emission lines of molecular hydrogen. Aspin et al. (1994) estimate the total luminosity of this object to be ≈ 1600 $L_\odot$.

Palla et al. (1994) obtained near infrared, CO, $C^{18}O$, CS, and H_2O maser observations on the group. Their high resolution VLA observations show that the maser source is clearly associated with LkHα 225-South. Moreover, a density concentration in the molecular cloud (as evidenced by CS J=5—4 emission) and a CO outflow are both associated with LkHα 225. In their model, LkHα 225 is at the center of a dense molecular core of mass ≈ 280 $M_\odot$, while BD+40°4124 lies near the periphery.

Hillenbrand et al. (1995) have obtained intermediate resolution optical spectra for all of the visible sources in the group. They classify BD+40°4124 as B2 Ve, LkHα 224 as B5 Ve, and both LkHα 225-North and South as mid-A to Fe. However, the luminosity of LkHα 255-South of

Send offprint requests to: P. R. Wesselius (p.r.wesselius@sron.rug.nl)

* Based on observations with ISO, an ESA project with instruments funded by ESA Member States (especially the PI countries: France, Germany, the Netherlands and the United Kingdom) and with the participation of ISAS and NASA

1600 $L_\odot$ (Aspin et al. 1994) puts this object well in the region of intermediate-mass stars.

In this paper, we present some initial results of ISO SWS observations towards three objects of the BD+40°4124 group. These spectroscopic observations allow us to probe the physical conditions in the vicinity of the star, and help restrict the applicable models for the infrared emission mechanisms.

2. Observations

In revolution 142 of ISO we observed LkHα 224 (at JD 2450181.960), LkHα 225 (JD 2450181.996) and BD+40°4124 (JD 2450182.037) with the SWS using observing mode 'S02'. A description of the SWS instrument and its observing modes is given elsewhere in this volume of A&A by de Graauw et al., whereas a full description of ISO itself is given by Kessler et al.. The employed SWS photometric and wavelength calibrations are also described elsewhere in this volume, by Schaeidt et al. and Valentijn et al., respectively. Each observation took about 45 minutes. BD+40°4124 was also observed in revolution 159 (at JD 2450198.635); both observations were combined.

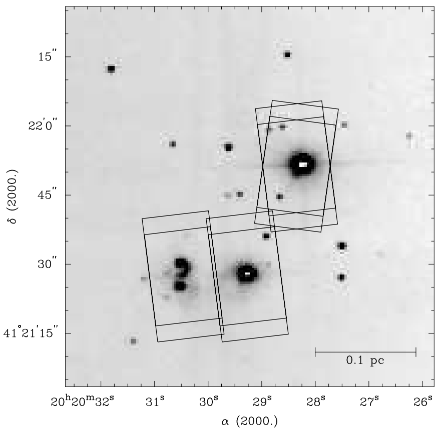

Fig. 1. SWS aperture positions for our measurements of (from right to left) BD+40°4124, LkHα 224 and LkHα 225 superimposed on a K-band image of the region. The large rectangles indicate the apertures for SWS bands 3A–3D (12.0–27.5 μm), whereas the smaller ones show the apertures for bands 1A–2C (2.4–12.0 μm)

Since SWS uses apertures that are fairly large compared to the separation of sources in most star forming regions, some caution is appropriate in interpreting such measurements. We created a plot with the positions of the SWS apertures, overlaid on a K-band image of the region (Hillenbrand, 1996, Fig. 1). Each aperture area just covers one of the three major sources which presumably are responsible for the H_2 emission.

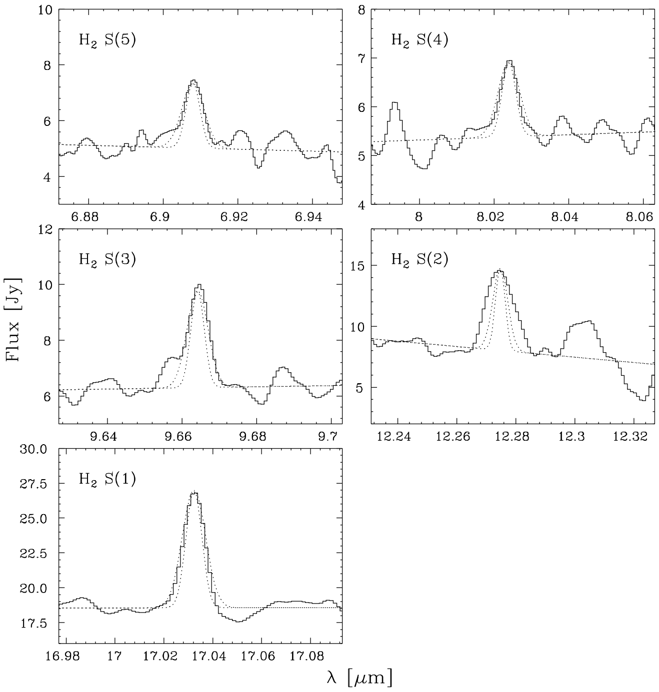

Fig. 2. Rotational H_2 lines detected in LkHα 224. Just for comparison, dotted lines are shown, indicate the instrumental resolutions for a point source and an extended source; for the flux determination the actually observed profile was used.

Of the pure rotational lines of H_2 we have only scanned the spectral regions of the lines S(0) to S(7), S(10), S(11) using 'S02'. This SWS observing mode makes it possible to detect narrow emission lines. The present dynamic range allows to detect a line flux of $\approx 5\%$ or more of the continuum, provided the continuum level is at ≈ 5 Jy or more. Line fluxes can be determined with an accuracy of about 30 % (Schaeidt et al. 1996). Because of instrumental problems (fringing) the S(2) line at 12.28 μm is more difficult to detect and measure (the one for LkHα 225 should be quite strong, but is lost in this fringing). Detected lines and measured line fluxes are listed in Table 1. Note that the detection of the S(4) line in BD+40°4124 is marginal, however. Plots of all detected lines, rebinned to a resolution $\lambda/\Delta\lambda$ of 3000 with an oversampling factor of four, are given in Figs. 2–4. The observed shape of the line profiles has rather large uncertainties at this stage of the data reduction: the broadening and P-Cygni profiles seen should be considered as artefacts at present.

The lines S(10) and S(11) were not detected in any of the objects. An upper limit on these line strengths, assuming they are unresolved, is 5×10^{-16} W m^{-2}.

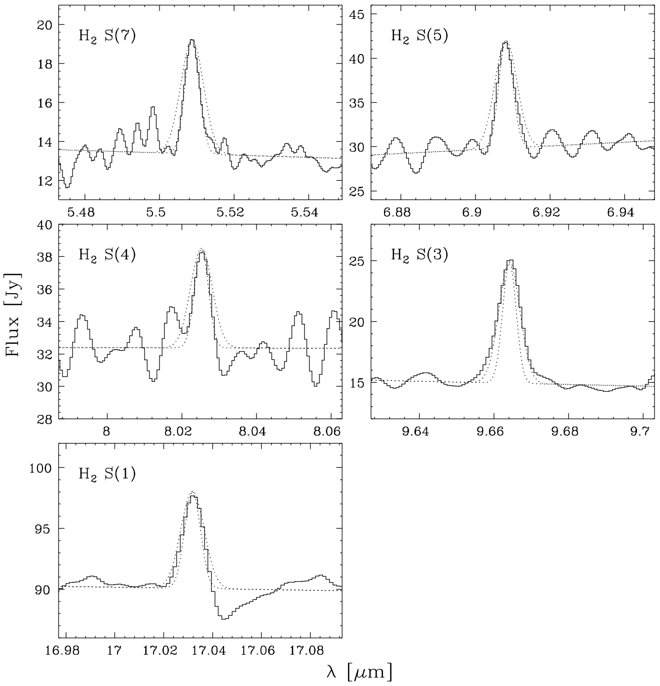

Fig. 3. The same as Fig. 2 for LkHα 225

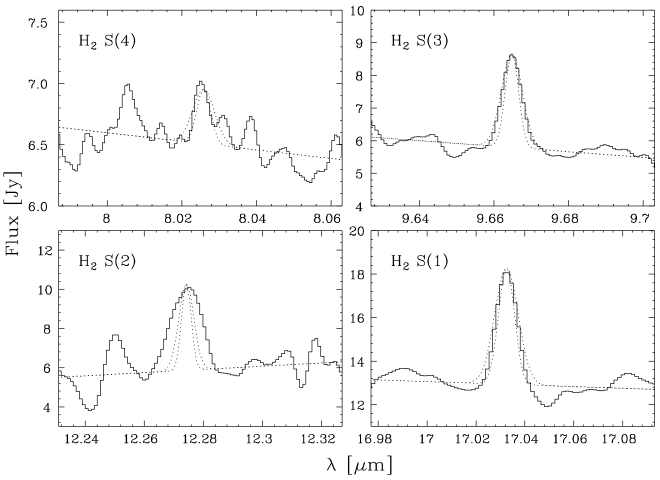

Fig. 4. The same as Fig. 2 for BD+40°4124

Table 1. Observed H_2 line fluxes (errors ≈ 30 %; 50 % for ':')

Object	Line	λ_c [μm]	Line Flux [10^{-16} W m^{-2}]	M (H_2) [$M_\odot$]
LkHα 224	S(5)	6.9084(5)	7.9	0.04
	S(4)	8.0241(5)	5.2	0.02
	S(3)	9.6648(5)	11.0	0.02
	S(2)	12.2747(8)	21.5:	0.05
	S(1)	17.0326(10)	13.0	0.02
LkHα 225	S(7)	5.5087(4)	39.2	0.3
	S(5)	6.9080(5)	48.8	0.02
	S(4)	8.0257(5)	18.3	0.02
	S(3)	9.6643(5)	28.4	0.02
	S(1)	17.0324(10)	13.2	0.02
BD+40°4124	S(4)	8.0254(8)	2.2:	0.02
	S(3)	9.6648(5)	8.3	0.01
	S(2)	12.2752(8)	6.1:	0.01
	S(1)	17.0325(10)	6.9	0.01

3. Discussion

That LkHα 225 is the dominant source of the BD+40°4124 group, as concluded by Aspin et al. (1994), is consistent with the continuum strength of these three objects: the SWS continuum in the range 5.5–17 μm is approximately 5 times higher at the position of LkHα 225 than at the two other pointings.

¿From the line fluxes listed in Table 1 it is possible to calculate the column densities in the upper J levels, averaged over the SWS beam, by using the A coefficients from Turner et al. (1977). For these objects, the extinction correction is particularly important for the S(3) line at 9.66 μm which is in the silicate absorption band. Aspin et al. (1994) derive an A_V of 25±9 magnitudes for LkHα 225-South, which would correspond to over one magnitude of extinction at the wavelength of the line. An examination of the continuum levels observed by the SWS is consistent with this level of extinction. Using the observed silicate absorption, we have applied an extinction correction with $A_V = 25^{\rm m}$ for LkHα 225, $20^{\rm m}$ for LkHα 224 and $10^{\rm m}$ for BD+40°4124. For the other wavelengths we have adopted a $1/\lambda$ extinction law.

A useful representation of the data is to plot the log of $N(\mathrm{J})/g$, the column density for a given J upper level divided by the statistical weight, versus the energy of the upper level (Fig. 5). Here the statistical weight is the combination of the rotational and nuclear spin components. We have assumed the high temperature equilibrium relative abundances of 3:1 for the ortho and para forms of H_2 . For a Boltzmann distribution, the slope of this plot is inversely proportional to the excitation temperature. Since the A-coefficients for the H_2 lines are quite small, these lines are optically thin and the excitation temperature will be close to the kinetic temperature of the gas.

Figure 5 supports this interpretation since all the line intensities for a given star can be well fit with a single temperature. That the points for ortho and para H_2 lie on the same line proves that our assumption on their relative abundances is correct. Other processes, such as UV pumping or the H_2 formation process, can affect the population distribution as well, but the data presented here show little evidence for this. Observations of higher excitation rotational lines and/or vibration-rotation lines are needed to better constrain these contributions.

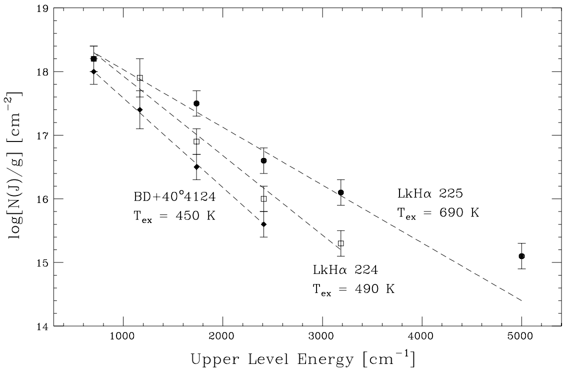

Fig. 5. H_2 excitation diagram for the BD+40°4124 objects

For BD+40°4124 and LkHα 224, the derived excitation temperature is approximately 500 K. The temperature of the H_2 gas for LkHα 225 is significantly higher, at nearly 800 K, if all the observed lines are considered. Just using the lowest four lines provides a significantly better fit (at 690 K); S(7) lies well above the fitted line. The excess emission in the highest J line could be the result of an additional contribution from formation-pumped emission. Additional observations of higher J-level transitions will be necessary to constrain the models.

Using the observed fluxes, assuming a thermal distribution of the low J levels, and correcting for the proposed extinction towards each of the objects, the average column density of the warm H_2 within the SWS beam has been estimated. Table 1 lists the results of this calculation for each line observed. The calculated values lie between 0.01 and 0.05 $M_\odot$ except for the deviating S(7) line of LkHα 225.

The rotational H_2 emission lines can originate from various distinct zones around the young stellar object (YSO), each excited by different processes. These include a scenario in which the photosphere of a circumstellar disk gets radiatively heated by the star and hence gives rise to emission rather than absorption lines. Alternatively, these lines may probe the inner (collapsing) envelope of the YSO where collisions with warm dust keep the gas to temperatures of 400–800 K. Radiation from the YSO may also create a photon-dominated region (PDR) in the surrounding molecular cloud where the gas is heated by photoelectrons ejected from grains (Burton et al. 1992). The required densities and FUV fields locate the PDR then fairly close to the YSO as well. Perhaps most likely, the H_2 emission originates in a very weak C-type shock wave driven into the surrounding molecular cloud by stellar outflows. Support for this interpretation comes from the paper by Aspin et al. (1994), who concluded that a source of shock-excitation must be present in the BD+40°4124 region.

Under the right conditions, all of these types of processes can give rise to very similar H_2 rotational emission spectra. Only complementary observations will be able to distinguish between them. Thus, circumstellar disks will have characteristic recombination line spectra, collapsing envelopes will radiate copiously in H_2O rotational lines, PDRs and shocks emit strong fine structure lines of [O I] and [C II] as well as rovibrational H_2 lines but their detailed spectra are quite distinct.

4. Conclusions

The SWS on ISO has been used to observe pure rotational lines of H_2 towards three young stellar objects in the BD+40°4124 group. The rotational population distributions are consistent with a thermal distribution in all three sources. The relative abundances of ortho and para H_2 are consistent with a high temperature equilibrium distribution. The flux in the S(3) line of LkHα 225 has to be corrected for ≈ 1.3 magnitudes of extinction due to the silicate absorption feature. Hence, the H_2 emission region for this embedded source appears to lie behind approximately $25^{\rm m}$ of A_V and could be associated with LkHα 225-South. For LkHα 224 and BD+40°4124 the pure rotational H_2 lines seem to be obscured by 20 and 10 magnitudes of visual extinction, respectively. An origin of these lines in a heavily obscured circumstellar disk seems unlikely because of the observed single temperature distribution and the very small amounts of H_2 involved. Therefore, these H_2 lines are probably not directly associated with the optical sources. The H_2 involved amounts to 0.01 to 0.04 $M_\odot$.

Acknowledgements. We thank the SWS operational team at VILSPA for their efforts to provide a calibration and data reduction system, suitable to produce this Letter. ETY acknowledges support under NASA grant NAGW-1285. We thank E.F. van Dishoeck and A.G.G.M. Tielens for many useful discussions and suggestions for improvements of this letter. L.A. Hillenbrand kindly provided the K-band image of the region shown in Fig. 1. We are grateful to J. Koornneef for a careful reading of the manuscript at a late stage.

References

Aspin, C., Sandell, G., Weintraub, D.A. 1994, A&A 282, L25
Burton, M.G., Hollenbach, D.J., Tielens, A.G.G.M. 1992, ApJ 399, 563
Cohen, M. 1972, ApJ 173, L61
de Graauw, Th., et al. 1996, this issue of A&A
Herbig, G. 1960, ApJS 4, 337
Hillenbrand, L.A. 1996, private communication
Hillenbrand, L.A., Strom, S.E., Vrba, F.J., Keene, J. 1992, ApJ 397, 613
Hillenbrand, L.A., Meyer, M.R., Strom, S.E., Skrutskie, M.F. 1995, AJ 109, 280
Kessler, M.F., et al. 1996, this issue of A&A
Palla, F., Testi, L., Hunter, D., et al. 1995, A&A 293, 521
Schaeidt, S., et al. 1996, this issue of A&A

Strom, K.M., Strom, S.E., Breger, M., et al. 1972, ApJ 173, L65
Turner, J., Kirby-Docken, K., Dalgarno, A. 1977, ApJS, 35, 281
Valentijn, E.A., et al. 1996, this issue of A&A
Weaver, W.B., Jones, G. 1992, ApJS 78, 239

This article was processed by the author using Springer-Verlag LaTeX A&A style file *L-AA* version 3.